Origins of the universal binding-energy relation

Amitava Banerjea* and John R. Smith
Physics Department, General Motors Research Laboratories, Warren, Michigan 48090-9055
(Received 26 October 1987)

The universality of the relation between binding energy and interatomic separation occurs for metallic and covalent bonds in a wide range of situations, spanning diatomic-molecule energetics, chemisorption, bimetallic adhesion, cohesion in solids, and even interactions in nuclear matter. This has intrigued physicists for some time, and here we provide some insights into its origin. We considered the electron density distribution as the variable linking the total energy and interparticle separation. In the spirit of effective-medium theory, a host electron density as seen by each atom was computed. We found that in every case (cohesion, chemisorption, and diatomic molecules), the host electron density was, to a good approximation, a simple exponential function of interparticle separation. This arises primarily because of the essentially exponential decay of the electron density into vacancy sites, into interstitial regions, into the vacuum from surfaces, or into the vacuum from isolated atoms. This suggested a scaling of the electron density which provides a universal relationship between the scaled interatomic separation and the scaled electron density. This density scaling is key. We applied the scaling of the electron density to impurity-binding-energy–host-electron-density curves computed via the effective-medium approximation. A universal energy–electron-density relationship resulted. This could be combined with the previously noted universal relation between scaled electron density and interparticle separation to yield the universal binding-energy–distance relation. First-principles values of cohesive energies of solids and the energetics of certain diatomic molecules were also correlated with host electron densities, despite the fact that these types of energies are fundamentally different from each other and from impurity binding energies. We found a universal relationship between energies and host electron densities for cohesion and certain diatomic molecules which was the same as the one discovered for impurity binding energies. This, together with the universal relationship between electron density and interatomic separation, helps one to understand how a *single* energy-distance relation could describe chemisorption and cohesion as well as diatomic energetics.

I. INTRODUCTION

A universal relation between the cohesive energy and the lattice constant of metals has been discovered.[1] The same universal form has also been shown to describe the relation between energy and separation in bimetallic adhesion,[1,2] metallic and covalent bonds in chemisorption[3] and in certain diatomic molecules,[4] and even nuclear matter.[5] (For reviews, see Ref. 6.) This universal relation has been extended beyond metallic cohesion to obtain[7] a universal equation of state (pressure-volume relation) for all classes of solids in compression and moderate expansion. It has been demonstrated[7] that the additional energy terms that lead to relations between total energies and interatomic spacings in ionic and van der Waals solids which differ qualitatively from those of metallic or covalent solids contribute only a slowly varying part to the pressure-volume (P-V) relation. Recently even finite-temperature effects, such as the temperature dependence of the thermal expansion in all classes of solids and the melting temperatures of metals, have been successfully treated[8] using the universal equation of state.

The universality of this relation between total energy and interatomic distance provides an intriguing unification between a number of phenomena which are apparently quite different. However, while there have been qualitative discussions about the origins of this universal behavior, no comprehensive explanation for it has yet been offered. The universal binding-energy relation (UBER) is valid over a wide range of phenomena and is also accurate—the agreement with experiment or first-principles theory is generally within the limits of experimental or theoretical error. As a consequence, any investigation of its origin must explain the breadth in its range of validity and also its accuracy. We do not claim to provide a rigorous derivation of the UBER, but rather a quantitative development which hopefully provides insight into its origin. We concentrate particularly on the UBER in the context of bulk cohesion of metals and covalently bonded solids, chemisorption on metal surfaces, and bonding in certain diatomic molecules.

We begin, in Sec. II, with a brief review of the UBER where we discuss the range of its validity as well as its limitations. In Sec. III we present a discussion of some general considerations regarding the origins of the UBER and lay out the broad outlines of our arguments. We concentrate on electron-density distributions as the quantities linking the total energy and interatomic spacings. In the next section, Sec. IV, we focus our attention on the UBER in the specific context of chemisorption of atoms

on metal surfaces. We note that there is a universal (exponential) form for the surface electron density as a function of the coordinate perpendicular to the surface. Next we consider the binding energy of impurities in uniform electron gases as a function of electron-gas density via the effective-medium theory proposed by Stott and Zaremba[9–11] and by Norskov and Lang.[12] Our universal electron-density–distance relation suggests a way to scale the total-energy–density relation. We find a universal energy–electron-density relation, which when combined with the universal density-distance relation yields our UBER. In Sec. V we discuss cohesion in bulk metals and covalently bonded solids, and consider diatomic molecules in Sec. VI. There we find universal relations between electron density and distance and between total energy and host-electron density which are identical in form to those found for chemisorption. These lead to a universal relationship between total energy and interatomic separation which is the same for chemisorption, cohesion, and diatomic energetics. We conclude with a summary and a general discussion in Sec. VII.

II. UNIVERSAL BINDING-ENERGY RELATION

The universality of the relationship between binding energy and atomic separation has been demonstrated by scaling the different binding-energy–distance curves onto the same universal curve by a simple procedure. We must point out that we are referring to variations of the *total* energy of the system as a particular length is varied and not to a pair-potential approximation. In all cases the energies are measured with reference to infinite separation between atoms in the case of cohesion and diatomic molecules, or between adsorbate and substrate in the case of chemisorption, or between metal surfaces in the case of bimetallic adhesion. We do not attempt to take the system through a phase transition such as the Mott transition, but rather consider energetics within phases. The prescription for scaling is simple,

$$E^*=E/\Delta E\ , \tag{1a}$$

$$a^*=(a-a_m)/l\ . \tag{1b}$$

Here E is the energy, a is the interatomic spacing, ΔE is the minimum value of the energy or the equilibrium binding energy, a_m is the equilibrium interatomic separation, and l is a scaling length. In the cases of cohesion in bulk metals and bimetallic adhesion, the scaling length was originally taken to be the screening length, but it is more conveniently and universally defined so that the second derivative of the scaled energy-distance curve is unity at equilibrium,

$$l=\left[\frac{\Delta E}{(d^2E/da^2)_{a_m}}\right]^{1/2}\ . \tag{2}$$

Figure 1 shows representative scaled energy-distance curves, $E^*(a^*)$, for cohesion, bimetallic adhesion, chemisorption, and a diatomic molecule. The range and accuracy of the UBER is clearly evident. It has been shown that the Rydberg function

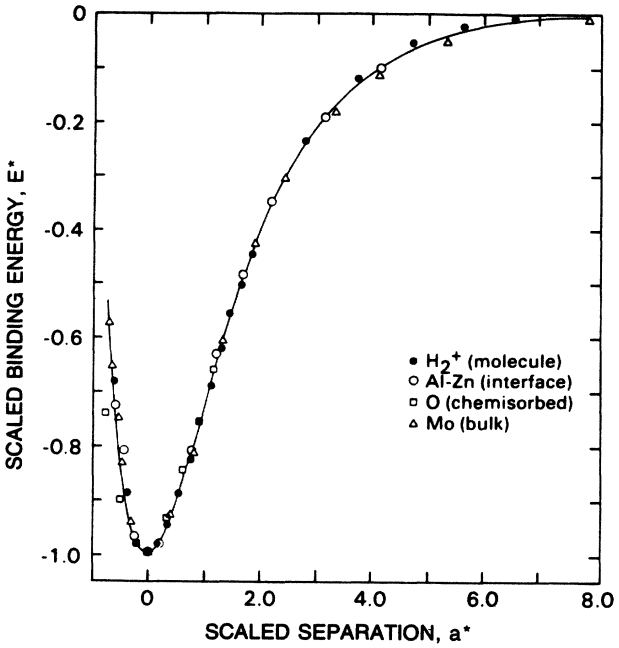

FIG. 1. Scaled binding energy E^* plotted against the scaled separation a^* for representative cases of cohesion, bimetallic adhesion, chemisorption at a jellium surface, and a diatomic molecule. The solid line is a plot of the Rydberg function. The sources of the unscaled results are listed in Fig. 1, Ref. 1.

$$E^*(a^*)=-(1+a^*)e^{-a^*} \tag{3}$$

is an accurate approximation to the UBER. The solid line in Figs. 1–4 is a plot of the function in Eq. (3). Figures 2–4 show similar plots of E^* versus a^* for bimetallic adhesion, cohesion, and chemisorption at a metallic

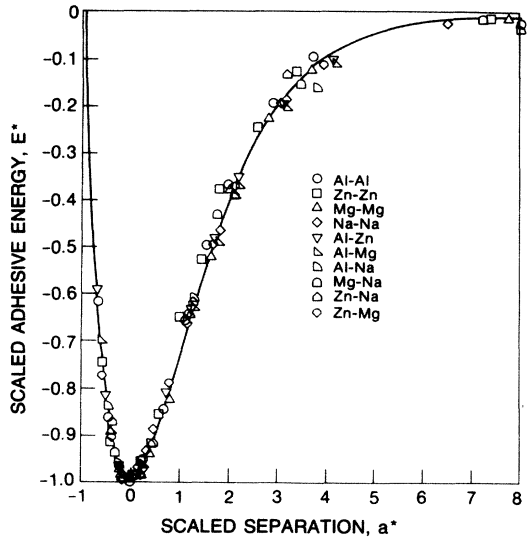

FIG. 2. Scaled adhesive energy E^* plotted against scaled separation a^* for representative metal pairs. The solid line is a plot of the Rydberg function. Unscaled adhesive energies are from Ref. 2.

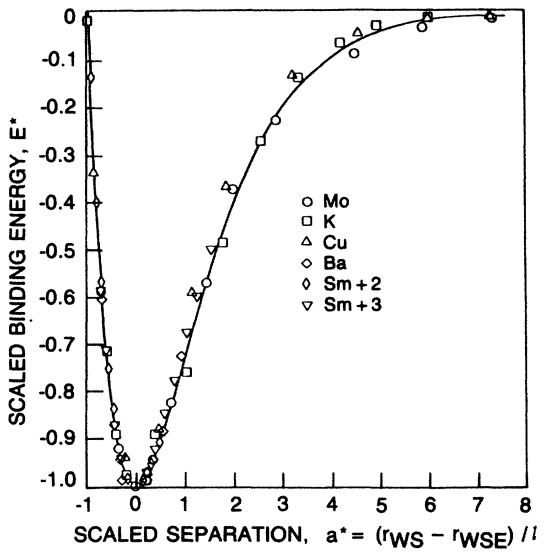

FIG. 3. Scaled cohesive energy E^* plotted against scaled interatomic separation a^* for representative solids. The solid line is a plot of the Rydberg function. The sources of the unscaled results are listed in Ref. 1.

surface. These show the universality of the UBER and that the plots in Fig. 2–4 are truly representative of their respective classes.

It has been realized that the origins of the particular form of the UBER and its universal character probably lie in the fact that, in all the cases considered, bonding results mainly from overlap of the tails of atomiclike wave functions. Hence, the UBER is not expected to apply in situations of ionic bonding between filled shells (e.g., alkali halides), or of van der Waals bonding. When atomic separations become very large, the overlap between atomic wave functions becomes small and the interaction between atoms becomes mostly of the van der Waals type. Thus the UBER is not expected to be valid at large interatomic spacings (on the far right of Fig. 1). On the other hand, when atoms are squeezed very close to each other, significant overlap may develop between their cores. One would expect the shell structure of the core to be element specific and so the UBER is likely not valid at very small interatomic spacing (on the far left of Fig. 1). At this juncture we must point out that the restriction to covalent and metallic bonding applied to UBER does not hold for P-V relation deduced from it. This is because even in ionic and van der Waals solids at equilibrium there is significant overlap between the "tails" of atomic wave functions centered on nearest neighbors. This suggests that for van der Waals solids in compression the effect of the overlap becomes dominant. For ionic solids in compression, the total energy is expected to be a sum of an overlap part, described by the UBER, and an ionic part. This ionic energy part varies more slowly with interatomic separation than the covalent energy and hence contributes a relatively constant term to the pressure whose variation with volume (or interatomic separation) is negligible compared to that of the pressure arising from the variation of the overlap energy. Consequently, on compression, when the overlap term is expected to become increasingly dominant, *the shape of the P-V relation is essentially the same for all classes of solids.*[7] This is also true for modest expansion, such as thermal expansion, as shown in Ref. 8. Nevertheless, it is well to keep in mind, as discussed above, that in cases where there is significant transfer of charge between different atoms, the contribution to the total energy arising from the interionic Coulomb interaction is in addition to the covalent or metallic (overlap) bonding that is described by the UBER.

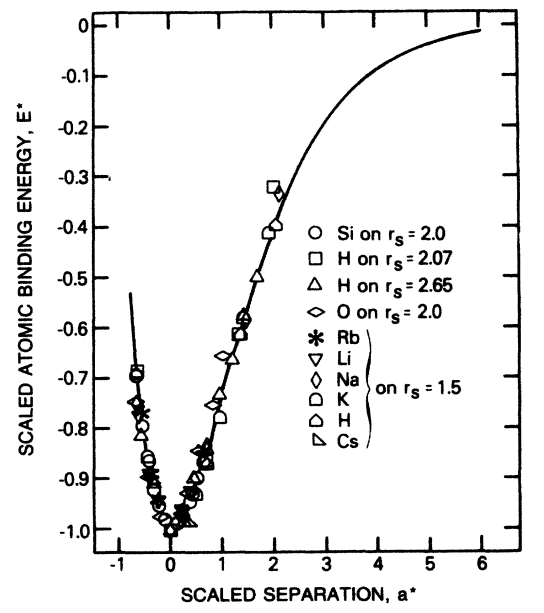

FIG. 4. Scaled binding energy E^* plotted against scaled separation (from the surface) a^* for representative cases of chemisorption on a metal surface. The solid line is a plot of the Rydberg function. See Fig. 3, Ref. 3 for the sources of the unscaled results.

A second point to remember is that universality in cohesion has been demonstrated only for cases where the crystal structure remains unchanged as the lattice constant is varied, i.e., for a "breathing" mode. This excludes such variations as crystal deformations that change the symmetry in a continuous fashion, as in shear, for example. While we will for the present omit such situations because the universality of binding-energy relations for such variations of interatomic separation has not been demonstrated, universality of binding-energy–distance relations in these situations cannot be ruled out. A related restriction applies in the case of chemisorption. The UBER has been demonstrated so far only for the case when the adsorbed atom is moved perpendicular to the plane of the substrate. We have formulated a method[13] which is as simple and convenient to use as the UBER for those cases where paths of atomic motions are not constrained. An example application might be the formation and propagation of cracks in solids. In this method lattice defect energies are deter-

mined via perturbation theory on a crystal whose lattice constant is chosen optimally. The crystal energies are given by the UBER, and the perturbation energy can be formulated simply.

One final point must be mentioned. The UBER has been demonstrated to be valid so far only when there are fermions shaping the underlying interactions in the system. In this vein, the UBER has been shown to be applicable, for instance, to nucleon-nucleon interactions and to a surface-energy–bulk-binding-energy relation in nuclear matter.[5] Here we will not concern ourselves with the UBER in the context of nuclear matter but will focus on cohesion in metals, chemisorption on metal surfaces, and diatomic molecule energetics subject to the limitations discussed above.

III. GENERAL CONSIDERATIONS

Before we begin considering the UBER in the specific context of one of the phenomena already mentioned, some general comments on its features are in order which illustrate the complexity of the challenge of determining the origin of the UBER. First, as the scaling is done [see Eqs. (1)], the scaling parameters are the equilibrium values of the energy and the curvature of the energy. That is, the energy-distance relations are assumed to be described by a two-parameter function given the equilibrium spacing. This is not necessarily true. Nevertheless, let us presume for the moment that a two-parameter function suffices. Of course each term in the energy expression must have the dimension of energy regardless of its dependence on length. For simplicity then, let us combine these two parameters into two new parameters, one of which has the dimension of length and the other has the dimension of energy. Hence, the scaling parameters can be conveniently chosen to be an energy and a length as has been done in Eqs. (1). Moreover, an *a priori* expectation that the energy-distance relation should be described by a two-parameter function is reasonable since the relation is so simple and smooth, as can be seen from Figs. 1–4. If the plot of energy against distance had a more wavy character or were not analytical (as might be the case through a phase transition), this expectation might be less reasonable. As it is, the fact that one can reproduce the anharmonic character of the relation by specifying only the harmonic part at the minimum, even when the curvature changes sign at separations not too far from the minimum, must be considered quite remarkable.

Some sense of the apparent complexity of the diverse phenomena covered by the UBER is obtained by noting that the relation between the cohesive energy and lattice constant in a transition-metal like molybdenum or copper has the same form as the binding-energy–distance relation for an oxygen atom chemisorbed on a simple metal like aluminum. The electrons involved in some material combinations are of s or p or hybridized s-p character, with the addition of d symmetry in some others, and even of f character in yet others. The mystery is that all such cases should behave in the same way as far as the energy-distance relation is considered. For instance, the characteristic ranges of electronic states with the different symmetry characters are quite varied and often the exponential tails of the electron clouds are characteristically preceded by a maximum. One might argue that the differences between different symmetries is largely obliterated by two effects. First, there can be significant hybridization between electrons of different symmetries. Also the total energy is an integral over all space of a functional of the total electron density and the integral tends to smooth out the differences between the different symmetries. Some of these points will be further clarified later in this paper.

While those arguments have some validity, we take the following approach to the problem. We consider the electron-density distribution as a primary variable, in keeping with density-functional theory.[14] The electron-density distribution is the link between the total energy and interparticle spacings. We first look for simple family functions which describe how the "host" electron densities (i.e., the electron densities seen by a given atom as produced by all *other* atoms in the system) depend on interparticle spacings. We then turn to the total energy as a function of electron density. Impurity embedding energies as a function of electron densities are obtained via the effective-medium approximation. Cohesive energies as a function of electron densities are obtained via augmented-spherical-wave[15] or relativistic Hartree-Fock[16] techniques. Total energies in the case of chemisorption and diatomic molecules are determined by a variety of other techniques. Thus when we find a universal relationship covering all of these phenomena, it is unlikely due to a particular theoretical approximation. This conclusion is further supported by numerous tests against experimental results (see, e.g., Refs. 1, 4, 7, and 8). We will see that the form of the universal scaling of the electron densities suggests a way to scale the relations between total energy and host-electron densities, leading to a universal relationship. When this relationship is combined with the universal form between host electron densities and interparticle spacings, we obtain the universal relation between total energy and interparticle spacing, which was our goal. Further, we find that the same universal forms for the relationship between host-electron density and distance and between total energy and host-electron densities apply to chemisorption, cohesion, and the energetics of certain diatomics. This is important to the understanding of why a single relationship between total energy and interparticle spacings applies to all of these phenomena.

We start by considering the case of chemisorption. We will first see that variation of the electron density outside a jellium surface with distance is of a simple exponential form for all jellium bulk densities. This suggests a simple exponential relationship between a^* and the scaled electron density n^*, as well as a scaling prescription to obtain n^*. Using this prescription, we then find that the variation of the embedding energy—in the effective-medium approximation—with host-electron (jellium) density is of the same form for all species of embedded atom. We argue that it is because the density-distance and energy-density relations are of universal form—the same for all

adsorbates and substrates—that the binding-energy–distance relations are universal. We further show that the universal binding-energy–distance relation that follows from combining the universal embedding-energy–electron-density relation and the universal jellium density-distance relation is the same as the UBER found in the original work.[1–6] We suggest that in the case of cohesion the cohesive energy can be correlated with local electron densities at more than one point in the host solid and that in the case of diatomic molecules the binding energy can be correlated with the local electron density of either of the two atoms. We examine two possible choices for the point in a bulk solid at which the electron density is evaluated, namely the center of a vacancy site and an interstitial point halfway between nearest neighbors.

All of these electrons densities vary in the same universal way with interatomic separation as the electron density from the jellium substrate varies with distance. We show that the relation between cohesive energy and electron density deduced for either of the two choices for the site in the bulk solid is of the same universal form as that found between embedding energy and host jellium density in Sec. IV and as that found between diatomic binding energy and the electron density of one of the atoms in Sec. VI. So, we conclude that the arguments put forward regarding the origin of universality in the binding-energy–distance relations in chemisorption also hold for cohesion in bulk solids and bonding in certain diatomic molecules.

IV. CHEMISORPTION

A. Effective-medium approximation

A simple method of computing the energies of impurities in solids has been proposed recently by Stott and Zaremba[9–11] and Norskov and Lang.[12] These authors realize, quite correctly, that a key to the total energy lies in a local electron density. Their method approximates the energy required to move the impurity from vacuum into the bulk as the energy of embedding the impurity atom in a homogeneous electron gas or jellium of the same density as the local host-electron density at the impurity site. These embedding energies need only be computed once for each species of impurity atom and then, knowing the host-electron density at the impurity site, the procedure involves simply looking up a number in a table of energies and electron densities. This estimate, referred to variously as the quasi-atom approximation, the effective-medium approximation, or the uniform density approximation, can be systematically improved upon by including the higher-order perturbative corrections to account for the fact that the electron density in the actual host is not uniform in the vicinity of the impurity. This method, which we shall hereafter refer to as the effective-medium approximation (EMA), has been successfully used to compute binding energies for vacancy entrapment of impurities in bulk metals[9,10] and for chemisorption on metal (jellium) surfaces.[9,12] In this section, we approach the energetics of chemisorption through the EMA. If the embedding energies as a function of host-electron density should have a complex form, then it would be unlikely that they could be simply scaled into a universal form.

The embedding energies for a number of atomic species have been computed and plotted as functions of the host jellium electron densities by a number of authors[11,12,14] using different methods within the local-density approximation (LDA). The plots of embedding energy versus host jellium density fall into two categories. Those for the inert gases show an almost linear rise in the energy with increasing density starting from zero energy at zero density. This is a reflection of the filled electron shells of these atoms and their consequent chemical inertness. The plots for all other atoms show an initial decrease in the embedding energy as the density increases. The energy then reaches a minimum and starts increasing, becoming large and positive at large densities. Overall, the plots for all these atoms look remarkably alike and are simple in form. This raises the question whether these plots reflect the same underlying functional relation between embedding energy E and jellium density n for all atoms (except, of course, the inert-gas atoms). In other words, one asks whether the curves for different atoms can all be simply transformed to one universal curve.

Tabular results for embedding energies as functions of jellium density were available for the computations of Stott and Zaremba[17] but not for those of Puska, Nieminen, and Manninen.[18] The difficulty with these data, as well as with some of the plots of Stott and Zaremba[10,11] is that for a number of atomic species the data and plots do not cover sufficiently low densities for the energy to reach the minimum. In the other cases, the number of data points in the regions of interest for the UBER, i.e., for negative energies, is too small to obtain a meaningful fit with any function.

As a result we had to resort to obtaining additional data by reading points off the published curves of Refs. 11 and 18. Those curves that did not reach the energy minimum, e.g., that for Be in Ref. 11, were ignored for the present purpose. The remaining curves, as obtained from the relevant publications, were photographically enlarged and points were read off the enlarged curves using a digitizing tablet connected to an IBM PC-AT computer. The data thus obtained were then smoothed by a least-mean-square spline-fitting procedure and finally usable data were generated by evaluating the spline function at a number of points in the relevant range. This is not a very accurate procedure, with the possibility of errors being introduced at every stage, but we felt that under the circumstances this was the best possible solution. A plot of the data thus generated compares very well with the original plots of Refs. 11 and 14. However, we also discovered that the results of the two groups (Refs. 9–11 and Ref. 14) can sometimes differ significantly. Nevertheless, as we will show below, we find that the different embedding-energy–electron-density curves can be described by the same functional form and scaled onto one universal curve.

It must be pointed out that we were not interested in all of the high-density, positive-energy portion of any

embedding-energy–electron-density curve since in practice it is difficult to reach such high compressions. These correspond to the far left of Fig. 1. The very-low-density part corresponds to the area on the far right of Fig. 1 and is the area where the LDA begins to fail and van der Waals effects start becoming important. Stott and Zaremba have noted this[11] and point out that their results are suspect for electron densities much lower than the value at the minimum. Consequently, we have concentrated on that portion of each curve which lies between about $n_m/2$ on the low-density side and $E_m/2$ on the high-density side, where the subscript m corresponds to the values at the energy minimum.

B. Surface electron densities

The EMA allows for a straight forward computation of the embedding energy given the host-electron density. Now we will concentrate on the computation of that electron density. It has been shown[1] that the electron-density distribution outside a jellium surface can be described by a universal function. In Ref. 1 the electron density and the distance were scaled by a simple prescription, analogous to Eqs. (1),

$$\tilde{n}=n/n_0\ ,$$
$$\tilde{a}=(a-a_m)/\lambda\ , \tag{4}$$

where a_m was taken to be zero (at the edge of the positive background), n_0 was set equal to n_+, the jellium density, and λ was taken to be the Thomas-Fermi screening length l_{TF}. It was shown that when so scaled, the variation of the electron density at a jellium surface was of a universal form for all bulk jellium densities, ignoring Friedel oscillations below the surface. It was further shown that a reasonable charge-conserving fit to the scaled data was

$$\tilde{n}=\begin{cases}(1-0.54e^{1.02\tilde{a}}), & \text{for } \tilde{a}<0\ ;\\ 0.46e^{-1.02\tilde{a}}, & \text{for } \tilde{a}>0\ .\end{cases} \tag{5}$$

Since typically the adsorbate does not penetrate between the surface atoms, for now we will consider $\tilde{a}>0$. Hence,

$$n=n_0\exp[-(a-a_m)/\lambda] \tag{6}$$

is an accurate representation of the electron density seen by adsorbates, where for Eq. (5) $n_0=0.46n_+$ and $a_m=0$. Because the relation is exponential, the values of n_0 and a_m are coupled but one of them can be chosen arbitrarily; that is, if n_0 and a_m are replaced by n_0' and a_0', with $n_0'=n_0\exp[-(a_0'-a_m)/\lambda]$, Eq. (6) remains unchanged. Therefore, we can conveniently choose a_m and n_0 to be the equilibrium distance and the substrate electron density n_m, respectively, at the equilibrium position for a particular adatom.

Electron-density distributions at surfaces and around other defects in real metals, including transition metals, can now be computed from first principles using, for example, the self-consistent local orbital method.[19] Here we choose a simpler approach. We simply overlap the electron densities of the constituent free atoms. (We have computed the free-atom electron densities within the LDA with Wigner correlation in a Herman-Skillman[20] scheme.) Our reasons are as follows. First, and foremost, we do not use these electron densities to compute other quantities such as total energies, but rather only aim to correlate computed chemisorption energies with them. Secondly, it turns out that this correlation is rather insensitive to the details of how the electron density is obtained. For example, we will see that in the case of cohesion in bulk metals either the interstitial or the vacancy site densities yield the same scaled energy-density relation to a good approximation.

Electron densities outside metal surfaces, obtained by this simple overlap of single-atom densities, can be fitted to the function in Eq. (6) and scaled in the same way as the jellium surface densities, i.e., using Eqs. (4). The scaled density-distance relations for some representative metals are shown in Fig. 5. We have computed surface densities as a function of z, the distance from the surface, for a number of metals at different symmetry points in the two-dimensional (100) unit cell of the surface as noted in the inset. We find that the fit to Eq. (6) is very good. This is true despite the fact that instead of a one-dimensional jellium surface we now have three-dimensional crystalline surfaces with not only s- and p-symmetry electron orbitals but also d orbitals.

It is important at this point to make a few further comments about our scheme of overlapping atomic densities. First, the contributions to the resultant net electron density from nearest- and next-nearest-neighbor (and farther) rings of atoms varies as z is changed, but the total density is not necessarily dominated by the nearest-neighbor contribution. The contribution from the other rings can be as large as half of the total. The other important point is that the effects of self-consistency and screening are expected to make the variation of density with distance smoother. Thus in some sense our approach of overlap-

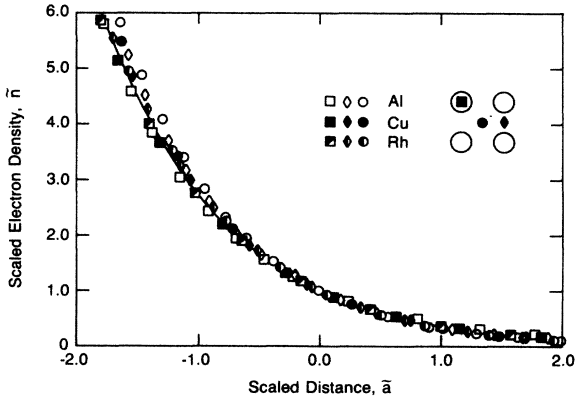

FIG. 5. Scaled electron density $\tilde{n}$ plotted against scaled distance from the surface $\tilde{a}$ for different sites on the (100) surfaces of Cu, Al, and Rh as noted in the inset. The solid line represents an exponential function $e^{-\tilde{a}}$. The origin, $\tilde{a}=0$, is taken 1.5 interplanar spacings toward the vacuum from a plane through the nuclei of the surface layer of atoms. The range in distance includes one interplanar spacing.

ping atomic electron densities provides a more difficult test for scaling than would the exact density distribution. Both of these observations will hold true for the case of a bulk solid when we consider the variations of a vacancy-site and an interstitial "bond-site" electron density with lattice constant in Sec. V.

If we presume then that the relation $n(a)$ has the same form for all metals surfaces, i.e., is universal, and if we can show that the relation $E(n)$ has the same form in all situations, i.e., for all atomic species, clearly the relation $E(a)$ must be of a universal form for all cases of chemisorption on a jellium surface. This will be our approach throughout this paper and we will show that there are universal functions $E^*(n^*)$ and $n^*(a^*)$ which are the same for chemisorption, cohesion, and certain diatomic molecules.

C. Free-electron gas $E(n)$

We will next give an example which suggests that the correct scaling procedure to obtain $E^*(n^*)$ is not straightforward. The total energy of a solid modeled as a crystalline array of positive-point charges immersed in homogeneous electron gas can be shown[21] to have the form

$$E = An^{2/3} - Bn^{1/3} , \tag{7}$$

where n is the electron density and A and B are known constants. The first term on the right-hand side arises from the electron kinetic energy and the second from electrostatic and exchange energies. The relation in Eq. (7) becomes more interesting when combined with Eq. (6),

$$E = A' e^{-2(a-a_m)/\lambda'} - B' e^{-(a-a_m)/\lambda'} \tag{8}$$

with

$$\begin{aligned} A' &= An_m^{2/3} = \Delta E , \\ B' &= Bn_m^{1/3} = 2\Delta E , \\ \lambda' &= 3\lambda = \sqrt{2}l , \end{aligned} \tag{9}$$

and a_m chosen so that $n_0 = n_m$. This form is identical to that of the Morse potential commonly used in the context of diatomic molecules and can be scaled to the dimensionless form

$$E^* = e^{-\sqrt{2}a^*} - 2e^{-a^*/\sqrt{2}} \tag{10}$$

with a^* defined as in Eq. (1b). The Morse function also is a good representation of the UBER depicted in Fig. 1.

Thus the form given in Eq. (7) appears to connect free-electron solids with diatomic molecules and as such becomes a prime candidate to test for a universal energy–electron-density relationship. Further, a plot of this energy function versus the density n has a form that at first sight appears remarkably similar to those of the embedding energy plots. This prompts one to further ask if the embedding energy curves are actually of the same form as for this model system. The function of Eq. (7) can be put into the dimensionless form

$$E^* = n_s^2 - 2n_s , \tag{11}$$

by scaling the electron density and energy in terms of the position and depth of the energy minimum

$$\begin{aligned} n_s &= \tilde{n}^{1/3} , \\ E^* &= E/\Delta E , \end{aligned} \tag{12}$$

where $\tilde{n}$ is defined by Eqs. (4) with $n_0 = n_m$ and where the position and depth of the minimum are given by

$$\begin{aligned} n_m &= \left[\frac{B}{2A} \right]^3 , \\ \Delta E &= \frac{B^2}{4A} . \end{aligned} \tag{13}$$

So the procedure is to compute ΔE and n_m via Eq. (13) for each atomic species whose embedding energies have been determined by the EMA, and then the $E(n)$ can be reduced to dimensionless form by scaling according to Eqs. (12). If Eq. (7) does indeed describe the data all the reduced points should lie directly on a plot of the function given in Eq. (11).

The results of this procedure are disappointing. The scaled relations are not at all close as can be seen from Fig. 6 which shows the scaled values of the embedding energies for nitrogen and oxygen as obtained from Refs. 11 and 18. The solid line in Fig. 6 is a plot of the function in Eq. (11). Clearly the function of Eq. (7) is not appropriate despite initial appearances.

Incidentally, Fig. 6 also shows apparent differences in the shapes of the curves obtained by the two independent groups. These differences are due to the two groups obtaining different results, but we will see that when the correct scaling procedure is brought forward the differences will be much smaller.

D. Universal function for $E(n)$

The failure of our attempt to scale the embedding-energy–electron-density curves onto the free-electron-gas energy-density curves compelled us to realize that (a) we were not using the right functional form to fit the curves, and/or (b) we were not scaling the variables in an ap-

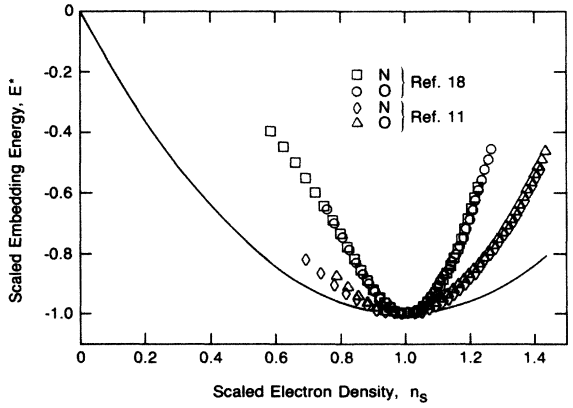

FIG. 6. Data obtained from Refs. 11 and 18 (as explained in the text) have been scaled according to Eq. (12). The solid line is a plot of Eq. (11).

propriate way. Let us first reexamine the scaling, Eq. (12). First, the scaling of E ($E^*=E/\Delta E$) is most certainly correct since it is exactly what was done to obtain the universal energy-separation relation [Eq. (1a)]. There is a problem with the density scaling, however, which is revealed by combining Eqs. (1b) and (6),

$$\tilde{n}=e^{-a^*l/\lambda} . \tag{14}$$

If there is to be a universal relationship between total energy and electron density, then there must be a one to one correspondence between the scaled electron densities and the scaled separations. This correspondence in fact would connect the universal energy–electron-density relation with the universal energy-separation relation. Clearly, Eq. (13) does not provide a one to one relationship, since the quantity

$$\gamma\equiv\lambda/l \tag{15}$$

could be expected to be different for different solids. The form of Eq. (6) does suggest a one to one scaling of the form

$$n^*=e^{-a^*} . \tag{16}$$

Combining Eqs. (6) and (16), we have

$$n^*=\left[\frac{n}{n_m}\right]^{\gamma} . \tag{17}$$

In analogy to the scaling of the distance in the UBER [see Eq. (2) and the discussion above it], the second derivative with respect to n^* of $E^*(n^*)$ at equilibrium is set equal to unity. This defines γ in terms of the second derivative of $E(n)$ at equilibrium through Eq. (17) as

$$\frac{1}{\gamma}=\frac{1}{n_m}\left[\frac{\Delta E}{(d^2E/dn^2)_{n_m}}\right]^{1/2} . \tag{18}$$

The analogy between the energy-separation scaling and energy-density scaling is obvious upon comparing Eqs. (18) and (2). In fact, combining Eqs. (2), (18), and (6) leads to Eq. (15) as it should.

Now let us carry out the scaling of the embedding-energy–electron-density curves of Refs. 11 and 18 according to Eqs. (17) and (18) and with $E^*=E/\Delta E$. The results are shown in Fig. 7 for some representative impurity elements. One can see that there is in fact a universal embedding-energy–electron-density relation. The solid line in Fig. 7 which represents the data well is of the form

$$E^*=-(1-\ln n^*)n^* , \tag{19}$$

with E^* defined as in Eq. (1a) and n^* defined through Eq. (17). Combining Eqs. (1a), (17), and (19), we have

$$E=-\Delta E\left[1-\gamma\ln\left[\frac{n}{n_m}\right]\right]\left[\frac{n}{n_m}\right]^{\gamma} . \tag{20}$$

As before, ΔE and n_m are the depth and electron density, respectively, at the energy minimum. Comparing Eqs. (20) and (7), we see that not only did we not have one-to-one scaling of the density in Sec. IV C, but we also did not have the correct functional form.

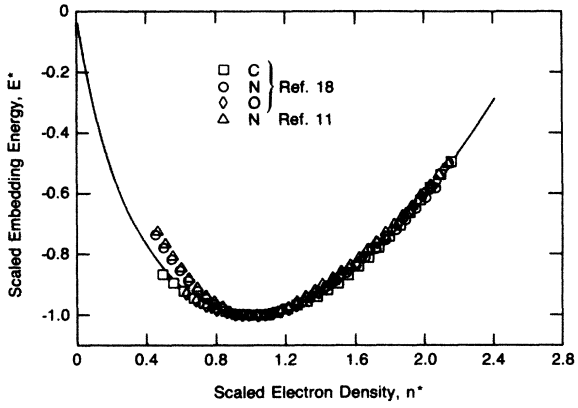

FIG. 7. Plot of scaled embedding energy against $n^*=(n/n_m)^{\gamma}$, where n is the electron density and n_m is the position of the minimum on the curve. Data obtained from Refs. 11 and 18 (as explained in the text) have been scaled according to Eq. (14) and $E^*=E/\Delta E$. The solid line is a plot of the function given in Eq. (19).

Another indication of the validity of the form in Eq. (20) which in fact takes us full circle back to Fig. 1 is found by combining Eq. (19) with Eq. (16). This yields Eq. (3) which is plotted as the solid line in Figs. 1–4. So we see that a combination of the universal energy–electron-density relation we obtained from the effective-medium approximation with the universal surface electron-density–distance relation yields the universal energy-separation relation. Putting it another way, the universal energy-separation relation is due to substrate electron densities being a simple exponential form in the vicinity of adsorbates and embedding energies being a universal function of host-electron densities. One could not have easily guessed the form of Eq. (20) and presumably that is why it had not been recognized that the embedding energies computed in the effective-medium approximation are of universal form.

We have come a long way now, but we still have quite a way to go. First, it is well known that the effective-medium approximation results we have used have inaccuracies. Secondly, we have so far considered only chemisorption, and we know that there is a single energy relation which ties together chemisorption, cohesion, and diatomic energetics. We will see that despite its inaccuracies, the effective-medium approximation gives the same $E^*(n^*)$ that is obtained from more accurate cohesion and diatomic calculations. Moreover, this is true even though we are comparing impurity embedding energies with cohesive energies and diatomic binding energies. Presumably, the inaccuracies of the effective-medium approximation are contained primarily in ΔE and $(d^2E/dn^2)_{n_m}$, and not in the *shape* of the $E^*(n^*)$. Presumably also the additional energy terms that differentiate between cohesion and embedding energies also are of the same, universal form as are the embedding energies to an accuracy sufficient that they can be scaled in the same way. We will deal with these and other questions in more detail in the remainder of this paper.

V. COHESION

A. Cohesive energies as a function of host-electron densities

As noted above, energies of cohesion are fundamentally different from impurity embedding energies. In cohesion, we assemble the solid from atoms that are originally isolated, as opposed to adding an impurity atom to an already assembled host. Cohesive energies must therefore be computed by methods different from effective-medium theory. Cohesive energies have been computed from first principles using various numerical methods as discussed below. Given the results of those computations, one might still wish to correlate them with a host-electron density where the host in this case for a given atom is all the other atoms in the elemental solid. In this way one makes a connection with the impurity or embedding problem, while making sure that the cohesive energies have been computed properly.

This electron density would of course vary with crystalline lattice constant. One might, in the spirit of the EMA, wish to take the host-electron density to be that found at the center of a vacancy. Alternatively, it might be argued that the relevant electron density is the electron density in the region where most of the interatomic bonding occurs, i.e., midway between nearest neighbors. Here we explore both possibilities. We will investigate the variation of the electron density with lattice constant at the two aforementioned sites. We will show that the variation with lattice constant of the electron density at either point does have the same form for all metals, or at least for the large number of metals tested, and that this form is that of Eq. (6). We will further show that the relation between cohesive energy and the electron density at either point has the same functional form for all the metals tested and that this form is the same as that of the relation between embedding energy and jellium density found in the previous section.

B. "Vacancy-site" electron density

Initially, as explained above, we concentrate on the vacancy-site electron density. This is the electron density n_v at a lattice site $\mathbf{R}_0$ which originates from atoms at all other sites $\mathbf{R}_i$, $i\neq 0$. Using the scheme of overlapping atomic electron densities, the "off-site" electron density at a lattice site may be written as

$$n_v = \sum_{i(\neq 0)} \rho(\mathbf{r}-\mathbf{R}_i) \ . \tag{21a}$$

Here, $\rho(\mathbf{r})$ is the free-atom electron density, $\mathbf{R}_i$ is the position of the ith atom, and the sum runs over all atomic sites except the one at the vacancy site, $i=0$. The Herman-Skillman free-atom electron density being spherically symmetric, this expression can be simplified to

$$n_v = \sum_{j=1}^{\infty} N_j \rho(d_j) \ , \tag{21b}$$

where N_j is the number of jth-neighbor atoms and d_j is the distance to the jth-neighbor atoms. Both $\{N_j\}$ and $\{d_j\}$ depend on the lattice structure of the solid in question.

We have computed the quantity n_v as a function of the lattice constant for a number of metals ranging from the simple metals, such as lithium and sodium, through the transition metals, such as nickel, to the noble metals, e.g., silver and gold. In order to exhibit the universal form of the variation of this electron density with lattice constant we initially scaled the density n_v and the lattice constant a for each metal to dimensionless quantities as in Eq. (4), with a_m the equilibrium lattice constant, $n_0 = n_v(a_m)$, and λ the Thomas-Fermi screening length (derived from n_0) of the metal in question. The results of this scaling are presented in Fig. 8 which shows plots of $\bar{n}$ versus $\bar{a}$ for some representative metals. The range of $\bar{a}$ in Fig. 8 and, indeed, in Figs. 9–11 as well, was chosen so that the volume per atom in the host crystal varied from 0.5 of the equilibrium value to 2.0 of the equilibrium value.

It is clear that the scaling is not very accurate. This is perhaps not surprising given the approximations made, particularly the use of the Thomas-Fermi scattering length. While that screening length worked well for jellium surfaces, clearly vacancies in, e.g., Ba or Rh are not closely represented by jellium surfaces.

The fits can be significantly improved by better choices for the parameter λ. With comparison to the situation of chemisorption in mind, we have tried to fit the values of $n_v(a)$ with an exponential function as in Eq. (6) allowing λ to vary. We have then scaled the values of $n_v(a)$ and a according to Eq. (4). The fits we have obtained are extremely accurate. Results of scaling with the optimized parameters are presented in Figs. 9 and 10. The improvement in the agreement is obvious. The optimum values of the parameters do not differ significantly from the original values for almost all of the metals examined. The solid line in Figs. 8–10 is the function $e^{-\bar{a}}$. That the points in Figs. 9 and 10 fall so closely on that line is indicative of how well the function in Eq. (6), which accurately described the electron-density distributions at jellium surfaces, also describes the vacancy electron-density distributions.

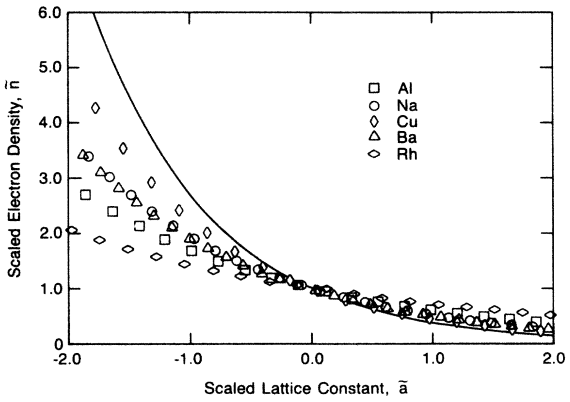

FIG. 8. Scaled electron density $\bar{n} = n_v/n_0$ plotted against scaled lattice constant $\bar{a}$ for some metals. The scaling length λ has been taken as the Thomas-Fermi scaling length l_{TF}. The solid curve is the function $e^{-\bar{a}}$.

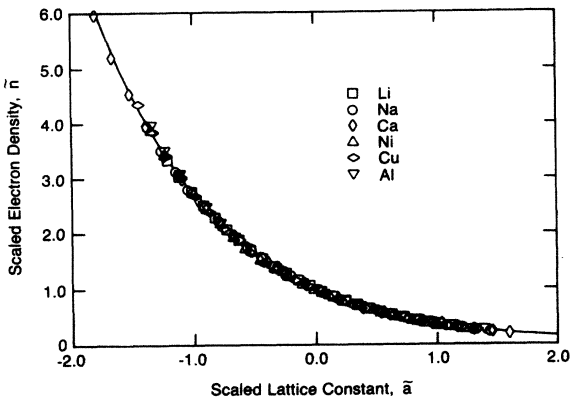

FIG. 9. Scaled density $\bar{n}=n_v/n_0$ plotted against scaled lattice constant $\bar{a}$ for some metals. The scaling length λ has been determined by optimizing a fit to an exponential function [Eq. (6)]. The solid curve is the function $e^{-\bar{a}}$.

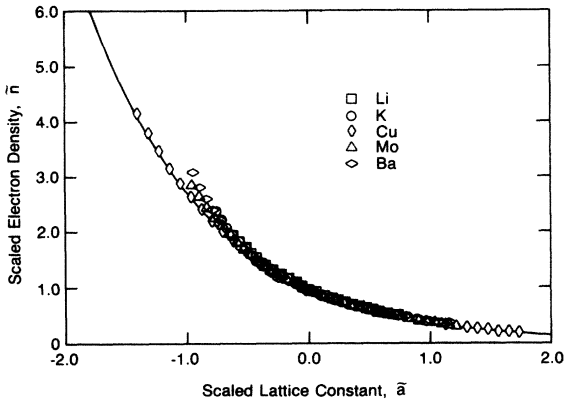

FIG. 11. Scaled density $\bar{n}=n_b/n_0$ plotted against scaled lattice constant $\bar{a}$ for some representative metals from Figs. 6 and 7. The scaling length λ has been determined by optimizing a fit to an exponential function [Eq. (6)]. The solid curve is the function $e^{-\bar{a}}$.

C. "Bond-site" electron density

One might argue that since cohesion is more like a process of interatomic bonding than of embedding a "self-impurity," the relevant density to correlate with the cohesive energy might be that in the bonding region, i.e., midway between nearest neighbors (with no vacancy introduced). We have investigated the variation of this bond-site electron density n_b with lattice constant in a number of a metals. We have computed n_b using the same approximation of overlapping atomic electron densities that was used in the previous section to compute the vacancy-site density. The values of $n_b(a)$ have been fitted with the exponential function of Eq. (6) and the values of n_b and a have been scaled as in Eqs. (4) using the equilibrium lattice constant a_m and the fitted parameters n_0 and λ. Once again, perhaps surprisingly, the fits are excellent. The scaled values $\bar{n}$ are plotted against the scaled lattice constant $\bar{a}$ in Fig. 11. The metals chosen for that plot are representative. Again the solid line is the function $e^{-\bar{a}}$. It is clear from this plot that the variation of n_b with a is very well described by the exponential function of Eq. (6) for all the metals considered, and so is of the same, universal form found for vacancies and at surfaces.

The exponential variation of the bond-site electron density is perhaps more surprising than that of the vacancy-site electron density. The bond-site density samples more of the inner reaches of the atoms (closer to the core), and might be expected to show deviations from exponential behavior. We have found, however, as evidenced in Fig. 11, that deviations from exponential behavior are not significant and the density distributions can be scaled together as long as one identifies the optimal scaling length. The value of this scaling length cannot be determined *a priori* because, since we are overlapping atomic densities, screening lengths are not necessarily the appropriate choice. Further, a screening length prescription for transition metals is less than clear.[22]

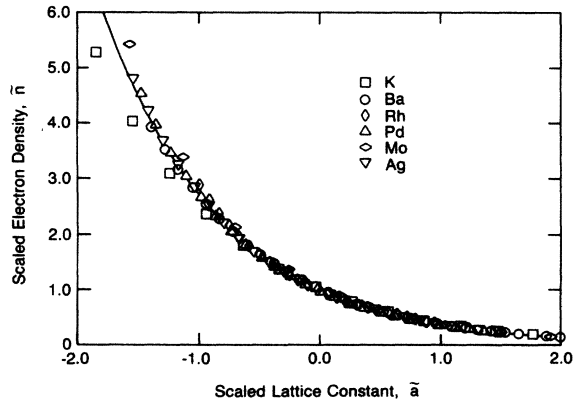

FIG. 10. Scaled density $\bar{n}=n_v/n_0$ plotted against scaled lattice constant $\bar{a}$ for some more metals. The scaling length λ has been determined by optimizing a fit to an exponential function [Eq. (6)]. The solid curve is the function $e^{-\bar{a}}$.

D. Correlation between cohesive energy and electron density

We have already discussed the possibility that the cohesive energy of the solid can be correlated with the electron density at a suitably chosen point in the crystal. Since we have, at this juncture, no theoretical basis for choosing the "best" site for such a correlation, we have tried to find an *ex post facto* one. We have used as our starting points the "raw" computed values of the cohesive energy as a function of lattice constant $E(a)$ and the variation of the electron density with lattice constant $n(a)$, where n is either the vacancy-site density n_v or the bond-site density n_b. From a knowledge of these we obtain the relation between cohesive energy and appropriate electron density $E(n)$. Now we can scale $E(n)$ according to Eqs. (17) and (18) and with $E^*=E/\Delta E$. The results are shown in Fig. 12 for the vacancy-site density. One

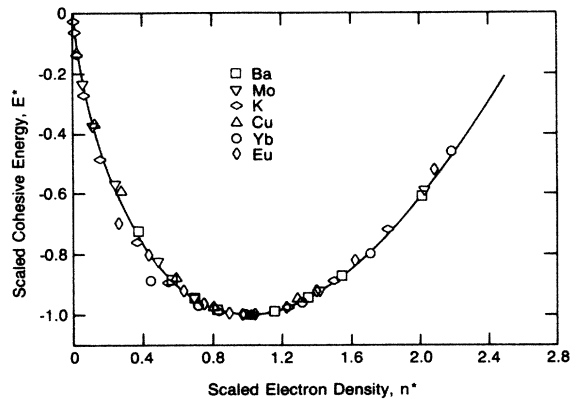

FIG. 12. Scaled cohesive energies for some metals plotted against $n^* = (n/n_m)^\gamma$. Vacancy-site densities n_v have been used for this plot. Similar results obtained using bond-site densities n_b are indistinguishable from those shown here after scaling. The solid line is a plot of the function given in Eq. (19).

can see first of all that there is a universal relationship between total energy and electron density. This is true even though now we have not only a simple metal (K), but also a noble metal (Cu), a transition metal (Mo), a band-overlap metal (Ba), and rare-earth metals (Yb,Eu). We find virtually an identical $E^*(n^*)$ when the bond-site density is used, and so it does not matter which of the two sites we choose as far as the scaling properties of $E(n)$ are concerned.

The solid curve is a plot of the expression given in Eq. (19). One can see that the agreement is excellent. Combining Eqs. (16) and (19), one obtains Eq. (3) which, as noted earlier, is the solid line in Figs. 1–4 and is clearly an accurate representation of the UBER. Again we have come full circle, and find that the universal relationship between cohesive energies and lattice constants is due to bond or vacancy electron densities being accurately described via a simple exponential family function [Eq. (6)], and to a universal relationship between cohesive energies and those electron densities. There is more. In comparison with Fig. 3, one must conclude that a single $E^*(n^*)$ describes both cohesion and impurity embedding. This helps explain how a single relationship between energy and interparticle separation can describe both cohesion and chemisorption. There are a few points that require further discussion. First, as mentioned earlier cohesion and embedding energies are fundamentally different. Added to this is the fact that while the effective-medium approximation has known inaccuracies, its $E^*(n^*)$ agrees well with that obtained via the more accurate cohesion calculations. The finding of a single $E^*(n^*)$ for both suggests that the differences are, to a surprising accuracy, of the same form in their dependence on the host-electron density. That is, one finds that the quantitative differences are primarily contained in ΔE and $(d^2E/dn^2)_{n_m}$. Finally, the cohesion results were obtained for host densities produced by a variety of s-, p-, and d-electron materials, while the effective medium is a free-electron gas. One must conclude that the effects of the effective-medium approximations and the variety of materials involved in cohesion are again found primarily in ΔE and $(d^2E/dn^2)_{n_m}$.

VI. DIATOMIC MOLECULES

The validity of the UBER in the context of diatomic molecules presents a new set of challenges. In some sense a diatomic molecule is the "most anisotropic" of the systems to which the UBER applies. The directionality of the bonding is very important. Although we did not discuss insulators and semiconductors in Sec. V while considering cohesion in a bulk solid, there is evidence[7] that the UBER applies to these solids too, although there are limitations as discussed below Eq. (3). These can be highly anisotropic solids with highly directional bonds. Rather strong anisotropies arising from the directional character of interatomic bonding can also be seen in transition metals which were discussed in Sec. V. Thus it would seem that the directionality of the bonding does not affect the universality of the binding-energy–distance relation. One reason for this is the total energy is an integral over all space of a functional of the electron density[14] which tends to average over the anisotropy of the electron density arising from the directional bonding. However, we have not as yet considered processes such as shear which could emphasize directional effects. While we will not consider the analogue of shear in the case of diatomics, the directional nature of the diatomic bond will be a significant test.

In one sense, the analysis of the energetics of diatomic molecules is simpler than for solids, because for the latter many atom forces come into play. In fact, the search for universal features associated with the molecular bond has been going on for quite some time. For example, Einstein[23] showed in his first two papers his early interest in universal principles by conjecturing on a universal nature of intermolecular interactions. This is in contrast to solids, where the first suggestion of universality appeared only recently.[1] The search for universality in diatomic molecule energetics has been a rich field, and for more recent references see Simmons, Parr, and Finlan.[24] Still, a scaling such as that of Eqs. (1) and (2) has not been suggested for diatomics. Recently, Graves and Parr[25] tested Eqs. (1) and (2) by comparing computed $(d^3E/da^3)_{a_m}$ and $(d^4E/da^4)_{a_m}$ with values calculated from spectroscopic data for 150 molecules from across the Periodic Table. This is the most difficult test yet for Eqs. (1) and (2) because up until then the highest derivative to be tested was the third (see Rose *et al.*[7]), and most testing had involved only the zeroth derivative of $E(a)$. As pointed out in Sec. II and elsewhere in the paper (see also Ref. 7), the UBER is expected to be valid only for metallic and covalent bonds, and not for ionic or van der Waals bonds. This is supported by Ref. 25. See particularly their Table I.

How shall we proceed in our attempt to understand universality in diatomic molecular energetics? Clearly we cannot use the effective-medium approximation as we did to understand chemisorption in Sec. IV, because the host

in the case of diatomics would be the other atom, hardly describable as a free-electron gas, even locally. On the other hand, we do wish to make a connection with chemisorption and cohesion and so perhaps we should proceed in a manner parallel to that followed for cohesion in Sec. V. That is, we will use state-of-the-art total energies and attempt to correlate them with host-electron densities.

As mentioned, the host-electron densities are in fact isolated atom electron densities. Our approach then is to investigate the scaling properties of isolated atom electron densities computed as described in Sec. V B. Scaling is carried out via Eq. (4), where the scaling parameters are determined by fitting the atom-electron density distributions to Eq. (6). The scaled electron-density distributions for isolated atoms are shown in Fig. 13. The solid curve is a plot of $e^{-\bar{a}}$. Clearly, the simple exponential form of Eq. (6) is an accurate description of the tail region of the atomic electron-density distribution, i.e., that part which is tailing off into the vacuum and which overlaps the other atom in making the diatomic bond. Remember that Eq. (6) also describes the tail region of the electron gas at metal surfaces and the vacancy and bond-site densities in bulk crystals. By comparing Fig. 13 with Figs. 9–11, one can see that the scaling is slightly better for the isolated atom than it is for the bond or vacancy sites in the solids. This is presumably because of next-neighbor and further-neighbor effects in the bond and vacancy sites, as discussed earlier.

Now we wish to correlate total energies $E(a)$ with these atomic densities by scaling according to Eqs. (17) and (18) with $E^*=E/\Delta E$. Note that because all atomic densities are of the form of Eq. (6), it does not matter whether we consider atom A to be the host for atom B in molecule AB or *vice versa*. We have carried out this correlation for a few diatomic molecules[26–28] and a few diatomic molecular ions.[29] The results are shown in Fig. 14. One can see that there is a universal relationship between the diatomic total-energy and host-electron density. The solid line in Fig. 14 is a plot of Eq. (19). One can see that it is an excellent representation of the $E^*(n^*)$ for diatomic molecules. Combining Eqs. (19) and (16), we obtain Eq. (3), which is plotted in Figs. 1–4. We can now understand the UBER for diatomics as being due atomic electron-density distributions being of a simple, exponential form and to a universal relationship between total energies and atomic electron densities. A comparison with Figs. 3 and 10 reminds us that this same $E^*(n^*)$ describes chemisorption and cohesion, respectively. This, together with the applicability of Eq. (6) to host-electron-density distributions in chemisorption, cohesion, and diatomic molecule energetics, helps us to understand how there could be a single relationship between total energies and interparticle separations for all of these phenomena.

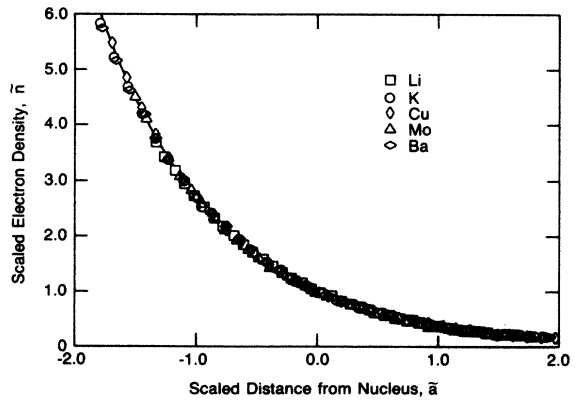

FIG. 13. Scaled free-atom density $\tilde{n}$ plotted against scaled distance $\tilde{a}$ from the nucleus for some atoms. The scaling length has been determined by optimizing a fit to an exponential function [Eq. (6)]. The solid curve is the function $e^{-\tilde{a}}$.

VII. DISCUSSION

We have presented some insights into why the relation between binding energy and interatomic separation should be universal in the separate contexts of bulk cohesion in solids, chemisorption of atoms on metal surfaces, and bonding in diatomic molecules. We saw that this universal relationship could be understood in terms of two findings. First, host-electron-density distributions, or electron densities seen by each atom in the molecule or solid, are accurately described by the simple, exponential family function given in Eq. (6) for chemisorption, cohesion, and diatomic molecules. Secondly, there is a universal relationship between this host-electron density and the total energy which is accurately represented by Eq. (19) for cohesion, chemisorption, and diatomic molecular energetics. Combining Eqs. (19) and (16) yields Eq. (3). This takes us full circle because, as shown in Figs. 1–4, Eq. (3) is an accurate representation of the universal relationship between total energies and interatomic separations.

Just as importantly as helping to understand why there is a universal relationship between total energies and interatomic spacings, we have reiterated the limitations of that relationship. It is limited to metallic and covalent bonds (fermions—with some evidence that this includes strong forces in nuclear matter). This limitation is lifted in the case of equations of state or pressure-volume relations for solids in compression or in thermal expansion. We apply the universal relation only within phases and not through phase transitions. Also the relative motions of the atoms are constrained to follow certain paths (e.g., fixed lattice structure in cohesion and chemisorbed atoms moving in same direction relative to surfaces). This is a limitation we[13] are attempting to overcome with a method of comparable simplicity to the universal energy relation, but we must go beyond the realm of applicability of the UBER to do it. Finally, it is perhaps useful to remind the reader that the UBER only provides the nonequilibrium behavior given ΔE and $(d^2E/da^2)_{a_m}$. One still needs to provide those two numbers from first-principles theory, experiment, or perhaps from simple empirical correlations.[30]

The EMA was used in our investigations of universality in chemisorption, and the approximation must, in all

practical cases, be corrected. Corrections are necessitated by two factors. First, one must correct for the fact that the electron density is not uniform. The second source of corrections is due to the fact that the hosts contain s, p, d, and f electronic symmetries. However the agreement between the $E^*(n^*)$ obtained via the EMA (Fig. 7) with that from cohesion (Fig. 12) and from diatomic energetics (Fig. 14) suggests that these corrections have little effect on $E^*(n^*)$ but rather apparently contribute primarily to ΔE and $(d^2E/dn^2)_{n_m}$. Thus they are not of direct importance to our understanding of the origin of the universality. Note also that the fact that the cohesive and diatomic binding energies are fundamentally different from impurity embedding energies also has little effect on $E^*(n^*)$. This suggests that the differences between these energies are also of the universal form to a reasonable accuracy.

Actually, we have carried the explanation of the UBER only a few steps along the way toward a complete understanding. One could ask why the host-electron-density distributions are of simple, exponential form. This is at least a reasonable result because wave functions decaying into vacuum are of this form. However, density distributions are due to a combination of many wave functions and so it is not obvious why this combination should be of such simple form. Further, it is not just due to atomic densities being of this form because more than one ring of neighbors contributes significantly to electron densities in cohesion and because the result holds even for jellium surfaces. One could also ask why total energies should be universal functions of host-electron densities. This is perhaps not as easy to understand or accept as exponential electron-density distributions. Those of us that are familiar with density-functional theory[14] are perhaps more comfortable thinking of the possibility of a universal relationship between total energies and electron densities than between total energies and interatomic spacings. The electron-density scaling relationship for the energy-density scaling was not obvious and was, in fact, suggested by the exponential form of the host-electron-density distributions. The plausibility of such an energy–electron-density relationship being of universal form is enhanced by the knowledge that the total energy is an integral of an energy density functional of the electron-density distribution which tends to average over

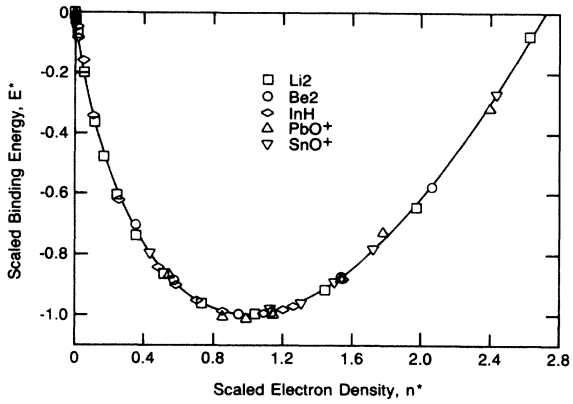

FIG. 14. Scaled diatomic binding energies plotted against $n^*=(n/n_m)^\gamma$. The solid line is a plot of the function given in Eq. (19).

density gradients and directional bonds. Further, hybridization tends to smooth s, p, d, or f electronic symmetry differences between the elements. Perhaps the most transparent reason for the universal energy–electron-density relationship is the simple form of the plot of energy versus electron density (Figs. 7, 12, or 14). These plots (see, e.g., Fig. 2 of Ref. 18) appear to have d^2E/dn^2 being of one sign (>0) for the range of densities considered. This is even a simpler form than the $E(a)$ plot shown in Fig. 1. Given such a simple form it is less surprising that requiring the values of the energy and its second derivative for various elemental systems to coincide at equilibrium leads to the curves coinciding over a substantial range of densities and energies.

ACKNOWLEDGMENTS

We gratefully acknowledge the cooperation of Professor M. J. Stott and Professor E. Zaremba who provided their tabular results on the embedding energies. We also are grateful to Professor Norskov for his suggestion that a possible connection existed between the effective-medium approach and the universal binding-energy relation. Finally, we acknowledge useful conversations with J. Ferrante and J. H. Rose.

*Present address: NASA Lewis Research Center, Cleveland, OH 44135.

[1]James H. Rose, John R. Smith, and John Ferrante, Phys. Rev. B **28**, 1835 (1983); Phys. Rev. Lett. **47**, 675 (1981).

[2]J. Ferrante and J. R. Smith, Phys. Rev. B **31**, 3427 (1985). See also John R. Smith and John Ferrante, Mater. Sci. Forum **4**, 21 (1985).

[3]John R. Smith, John Ferrante, and J. H. Rose, Phys. Rev. B **25**, 1419 (1982). See also John P. Perdew and John R. Smith, Surf. Sci. Lett. **141**, L295 (1984).

[4]John Ferrante, John R. Smith, and James H. Rose, Phys. Rev. Lett. **50**, 1385 (1983).

[5]James H. Rose, James P. Vary, and John R. Smith, Phys. Rev. Lett. **53**, 344 (1984).

[6]John R. Smith, James H. Rose, John Ferrante, and Francisco Guinea, in *Many-Body Phenomena at Surfaces,* edited by D. Langreth and J. Suhl (Academic, New York, 1984), pp. 159–174; John R. Smith, John Ferrante, P. Vinet, J. G. Gay, R. Richter, and J. H. Rose, in *Chemistry and Physics of Fracture,* edited by R. H. Jones and R. M. Latanision (Nijhoff, Netherlands, 1987), pp. 329–362.

[7]P. Vinet, J. Ferrante, J. R. Smith, and J. H. Rose, J. Phys. C **19**, L467 (1986); J. Geophys. Res. **92**, 9319 (1987). See also J. H. Rose, J. R. Smith, F. Guinea, and J. Ferrante, Phys. Rev. B **29**, 2963 (1984).

[8]P. Vinet, J. R. Smith, J. Ferrante, and J. H. Rose, Phys. Rev. B

35, 1945 (1987). See also F. Guinea, J. H. Rose, J. R. Smith, and J. Ferrante, Appl. Phys. Lett. **44**, 53 (1983).

[9]M. J. Stott and E. Zaremba, Solid State Commun. **32**, 1297 (1979).

[10]M. J. Sott and E. Zaremba, Phys. Rev. B **22**, 1564 (1980).

[11]M. J. Stott and E. Zaremba, Can. J. Phys. **60**, 1145 (1982).

[12]J. K. Norskov and N. D. Lang, Phys. Rev. B **21**, 2131 (1980).

[13]John R. Smith and Amitava Banerjea, Phys. Rev. Lett. **59**, 2451 (1987); *ibid.* (to be published).

[14]P. Hohenberg and W. Kohn, Phys. Rev. **136**, B864 (1964). See also W. Kohn and L. J. Sham, *ibid.* **140**, A1133 (1965).

[15]A. E. Carlsson, C. D. Gelatt, and H. Ehrenreich, Philos. Mag. A **41**, 241 (1980).

[16]J. F. Herbst, Phys. Rev. B **24**, 608 (1981); J. F. Herbst and J. W. Wilkins, *ibid.* **24**, 1679 (1981).

[17]M. J. Stott and E. Zaremba (private communication). For plots of these results see Refs. 10 and 11.

[18]M. J. Puska, R. M. Nieminen, and M. Manninen, Phys. Rev. B **24**, 3037 (1981).

[19]John R. Smith, Jack G. Gay, and Frank J. Arlinghaus, Phys. Rev. B **21**, 2201 (1980).

[20]Frank Herman and Sherwood Skillman, *Atomic Structure Calculations* (Prentice-Hall, Englewood Cliffs, 1963).

[21]See, e.g., N. W. Ashcroft and N. D. Mermin, *Solid State Physics* (Holt, Rinehart, and Winston, New York, 1976), pp. 410–413.

[22]For a more detailed discussion of this point see, for example, Ref. 1.

[23]A. Einstein, Ann. Phys. (Leipzig) **4**, 513 (1901); **8**, 798 (1902).

[24]G. Simons, R. G. Parr, and J. M. Finlan, J. Chem. Phys. **59**, 3229 (1970).

[25]John L. Graves and Robert G. Parr, Phys. Rev. A **31**, 1 (1985).

[26]I. Schmidt-Mink *et al.*, Chem. Phys. **92**, 263 (1985).

[27]B. H. Lengsfield *et al.*, J. Chem. Phys. **79**, 1891 (1983).

[28]C. Teichteil and F. Spiegelmann, Chem. Phys. **81**, 283 (1983).

[29]K. Balasubramanian, J. Phys. Chem. **88**, 5759 (1984).

[30]See, e.g., J. Gerkema and A. R. Miedema, Surf. Sci. **124**, 351 (1983), and references therein.